Available online at www.sciencedirect.com
SCIENCE DIRECT
Cement and Concrete Research 35 (2005) 85–98
CEMENT AND CONCRETE RESEARCH

Synthesis and characterisation of magnesium silicate hydrate gels

D.R.M. Brew, F.P. Glasser*

School of Engineering and Physical Sciences, University of Aberdeen, 033 Meston Building, Aberdeen AB24 3UE, Scotland, UK

Received 5 February 2003; accepted 4 June 2004

Abstract

Magnesium silicate hydrate gels (M-S-H) have been prepared by precipitation. The range of gel compositions lie between Mg/Si molar ratios 0.67–1.0. The gels were subject to short cure, approximately 24 h at approximately 22 °C and longer cure, 180 days at 85 °C, following which they were characterised by XRD, FT-IR and solid-state ^{29}Si NMR. Ageing at longer times and higher temperatures somewhat improves the local ordering. The nature of the partially ordered structures is related to those of M-S-H mineral phases. The structures and compositions of M-S-H gels differ from those of C-S-H gels and partly on that account, C-S-H gels contain little magnesium while M-S-H gels in blended cements coexist with C-S-H but contain little calcium.

Keywords: MgO–SiO_2–H_2O gels; MgO–SiO_2–H_2O minerals; ^{29}Si NMR, FT-IR; Gel structures

1. Introduction

While the MgO content of Portland cement is typically low, 1–4%, addition of iron blast furnace slag may substantially increase the bulk magnesia content of the resulting blend. However, even cements with low initial magnesia contents may react with Mg-containing ground waters, as a result of which, several MH and magnesium silicate hydrate (M-S-H) phase(s) form. Brucite, $Mg(OH)_2$, is often reported as a reaction product. Another product of reaction has been identified as an M-S-H phase having Mg/Si ratios ranging between 4:1 and 1:1 [1–3]. Gollop and Taylor [4] characterised this product as a poorly crystallized serpentine, approximately $M_3S_2H_2$.

In the present study, a Portland cement has been exposed to $MgSO_4$ solution for 6 months and the reaction products characterised. The exposure was at 85 °C to accelerate reaction relative to control samples, at 25 °C. The exposure tests were complimented by synthesis and characterisation of M-S-H gels made from reagent grade chemicals at both 20–25 °C and 85 °C using a combination of techniques: solid-state ^{29}Si *n*uclear *m*agnetic *r*esonance (NMR) to determine local structural organisation; powder *X-r*ay *d*iffraction (XRD) to observe the development of crystallinity; as well as *F*ourier *t*ransform-*i*nfra*r*ed spectroscopy (FT-IR) and electron microscopy using an *e*nergy-*d*ispersive *X*-ray analytical system (EDX) to corroborate NMR evidence and check for product homogeneity.

2. Experimental

The term *gel*, while normally used to describe nearly amorphous materials, such as silica gel, is used here to describe precipitated M-S-H phases of low crystallinity; these are structurally intermediate between a true gel and a crystalline phase or phases. M-S-H gels were precipitated as follows. Stock solutions of sodium metasilicate, $Na_2SiO_3{\cdot}5H_2O$ (METSO 510, Na/Si = 1.0, Crosfield, UK) and of $Mg(NO_3)_2{\cdot}6H_2O$ (AnalaR, BDH, UK) were prepared. The required solution volumes to achieve five selected Mg/Si target ratios were cooled to about 0 °C and mixed with stirring in a three-necked round-bottomed flask kept immersed in an ice-water bath. The sodium silicate solution was added first, followed by slow addition of the magnesium solution. Inhomogeneous coprecipitation was minimised by (1) the order of addition, keeping reaction conditions alkaline

* Corresponding author. Tel.: +44-1224-272-906; fax: +44-1224-272-908.
E-mail address: f.p.glasser@abdn.ac.uk (F.P. Glasser).

0008-8846/$ – see front matter © 2004 Elsevier Ltd. All rights reserved.
doi:10.1016/j.cemconres.2004.06.022

Table 1
Target and observed Mg/Si ratios for synthetic M-S-H gels

M-S-H gel	Curing conditions	Target Mg/Si ratio	Number of analyses by EDX	Mean Mg/Si ratio ($\bar{x}$) by EDX ($\bar{x} \pm \sigma$)
Fresh M-S-H gels				
1	24 h at 20–25 °C	0.50	20	0.66 ± 0.10
2	24 h at 20–25 °C	0.60	25	0.75 ± 0.19
3	24 h at 20–25 °C	0.75	26	0.80 ± 0.15
4	24 h at 20–25 °C	1.00	24	0.90 ± 0.07
5	24 h at 20–25 °C	1.50	20	0.96 ± 0.16
Aged M-S-H gels				
6	6 months at 85 °C	0.50	21	0.82 ± 0.04
7	6 months at 85 °C	1.00	23	0.86 ± 0.07
8	6 months at 85 °C	1.50	21	0.89 ± 0.05
9	6 months at 85 °C	2.00	22	0.94 ± 0.05

throughout the precipitation process and (2) constantly stirring the reaction mixture. The composition was allowed to warm to ambient, 20–25 °C, and the precipitate settled readily leaving a clear supernatant solution.

An aliquot of the supernatant was removed by pipette and analysed for Na and unreacted Mg and Si using flame emission and atomic absorption spectroscopy, as well as UV/visible spectrophotometry, for Na, Mg and Si, respectively. The precipitate was filtered using a Büchner filter funnel kept in an N_2-filled AtmosBag (Aldrich, UK). The solids were washed five times with a large volume of double distilled, deionised water (1000 ml) to remove residual sodium. Each wash was analysed for Na. The fifth wash from all preparations had a $[Na^+] < 50$ ppb, which was at the detection limit of the flame emission spectrometer. Subsequent analysis of the solids using EDX analysis did

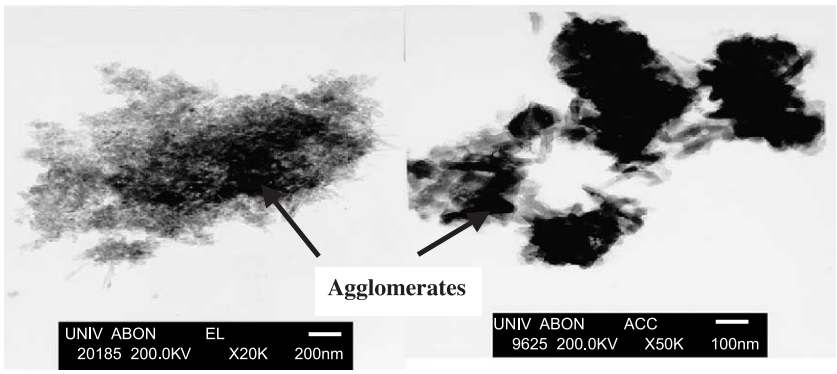

Fig. 1. Transmission electron micrograph of M-S-H Gel 4. Note the agglomerated structure.

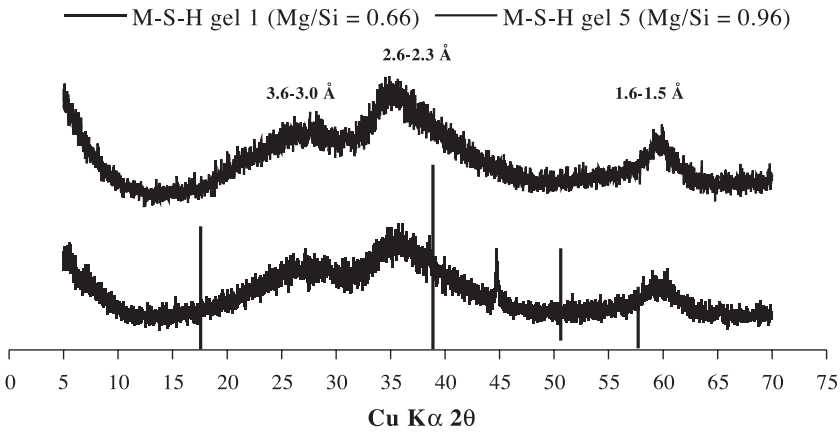

Fig. 2. XRD spectra of M-S-H Gels 1 and 5. The peak near 45°2θ is an artefact due to the sample holder. Vertical black lines denote the major reflections for $Mg(OH)_2$ and their relative intensities.

Table 2
Chemical analyses data of supernatant and EDX data for synthetic M-S-H gels

M-S-H gel	Target Mg/Si ratio	Mean Mg/Si ratio by EDX[a] ($\bar{x} \pm \sigma$)	Range of Mg/Si ratios[b]	Final [Mg^{2+}] (mM)[c]	Final [Si^{4+}] (mM)[c]
1	0.50	0.66 ± 0.10 (20)	0.49–0.83	6.6	35.8
2	0.60	0.75 ± 0.19 (25)	0.35–1.03	4.8	28.1
3	0.75	0.80 ± 0.15 (26)	0.36–0.93	1.0	6.5
4	1.00	0.90 ± 0.07 (24)	0.82–1.03	10.0	11.8
5	1.50	0.96 ± 0.16 (20)	0.78–1.53	14.1	3.5
M-S-H gels aged for 6 months at 85 C					
6	0.50	0.82 ± 0.04 (21)	0.73–0.87	6.5	21.9
7	1.00	0.86 ± 0.07 (23)	0.72–1.02	4.4	61.8
8	1.50	0.89 ± 0.04 (21)	0.79–0.95	23.3	0.6
9	2.00	0.94 ± 0.06 (22)	0.80–1.12	42.6	29.6

[a] Number of particles analysed in parentheses.
[b] By EDX of micron-sized regions.
[c] Supernatant liquid molarities.

not reveal signals attributable to sodium. The product was placed onto a watch glass and moist dried over solid $CaCl_2$ (AnalaR, BDH) at room temperature, 20–25 °C for approximately 5–7 days until ready for use. Throughout the paper, this preparation of M-S-H gels is referred to as "fresh" gels. A second series of reaction product having target Mg/Si ratios of 0.5, 1.0, 1.5 and 2.0 were prepared at 20–25 °C and subsequently stored in double-distilled, deionised water for 6 months at 85 °C to examine the effects of ageing: these are referred to as "aged" gels.

NMR is useful to determine the state of silicon polymerisation. The observed ^{29}Si NMR resonances for M-S-H minerals are normally in the Q^3 chemical shift range unless significant cationic substitution has occurred. Contact times

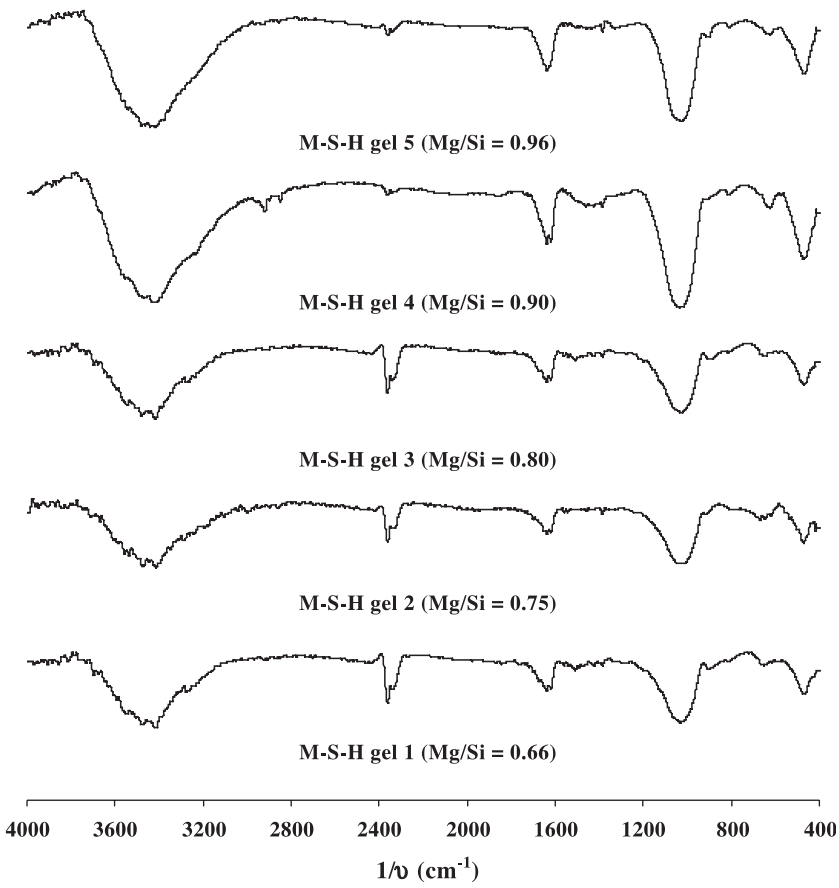

Fig. 3. FT-IR spectra of M-S-H Gels 1–5. Each sample was mixed with KBr and pressed. Absorptions near 2400 cm^{-1} are artefacts due to air contamination.

Table 3
FT-IR data for M-S-H Gels 1–5

M-S-H gel (Mg/Si)	OH vibrations (cm^{-1})	Si–O vibrations (cm^{-1})	Mg–O vibrations (cm^{-1})
1 (0.66)	3676 **w** (str)	1214 **w** (Q^3 str)	640 **w** (bdg)
	3410 **s** (H-bond, str)	1054, 1017 **s** (Q^2 str)	472 **w** (str)
	1622 **m** (str)	904 **w** (Q^2 bdg)	432 **m** (bdg)
		788, 687 **w** (Q^1 bdg)	
2 (0.75)	3713 **w** (str)	1225 **w** (Q^3 str)	551 **m** (str)
	3414 **s** (H-bond, str)	1014 **s** (Q^2 str)	472 **m** (str)
	1620 **m** (str)	914 **w** (Q^2 bdg)	417 **m** (str)
		778, 670 **w** (Q^1 bdg)	
3 (0.80)	3696 **w** (str)	1228 **w** (Q^3 str)	470 **m** (str)
	3418 **s** (H-bond, str)	1079, 1029 **s** (Q^2 str)	
	1620 **m** (str)	902 **w** (Q^2 bdg)	
		813 **w** (lattice str)	
		650 **w** (Q^1 bdg)	
4 (0.90)	3671 **w** (str)	1212 **w** (Q^3 str)	473 **m** (str)
	3418 **s** (H-bond, str)	1082, 1033 **s** (Q^2 str)	
	2919, 2850 **w** (str)	911 **w** (Q^2 bdg)	
	1620 **m** (str)	812 **w** (lattice str)	
		622 **w** (Q^1 bdg)	
5 (0.96)	3688 **w** (str)	1207 **w** (Q^3 str)	534 **w** (str)
	3403 **s** (H-bond, str)	1040, 1017 **s** (Q^2 str)	476 **m** (str)
	1618 **m** (str)	950, 898 **w** (Q^2 bdg)	
		624 **w** (Q^1 bdg)	

Key: **s**—strong; **m**—medium; **w**—weak; str—stretching vibration; bdg—bending vibration.

and pulse delays of 1 ms and 3 s, respectively, were appropriate to observe all potential silicon sites. An additional single delay of 60 s was used to confirm the presence or absence of Q^4 species. Approximately 3000 accumulations were acquired for each spectrum to give acceptable signal/noise ratios.

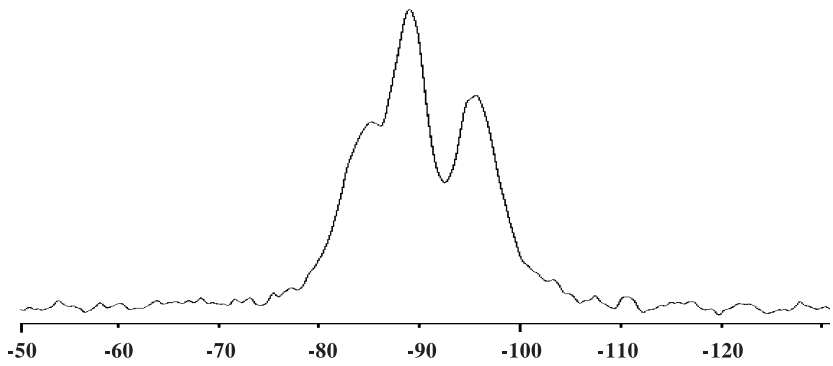

Fig. 4. ^{29}Si MAS NMR spectrum of M-S-H Gel 1 (Mg/Si = 0.66).

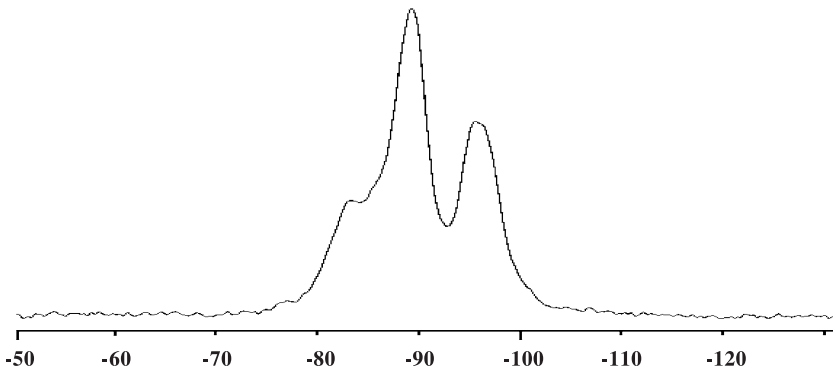

Fig. 5. $\{^1H-^{29}Si\}$ CP-MAS NMR spectrum of M-S-H Gel 1 (Mg/Si = 0.66).

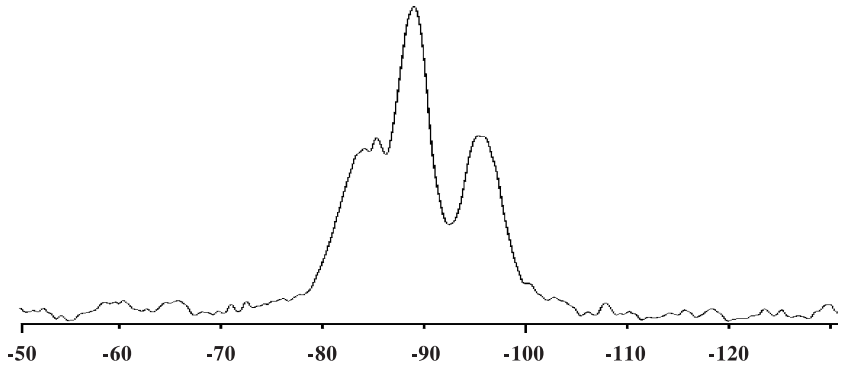

Fig. 6. ^{29}Si MAS NMR spectrum of M-S-H Gel 2 (Mg/Si = 0.75).

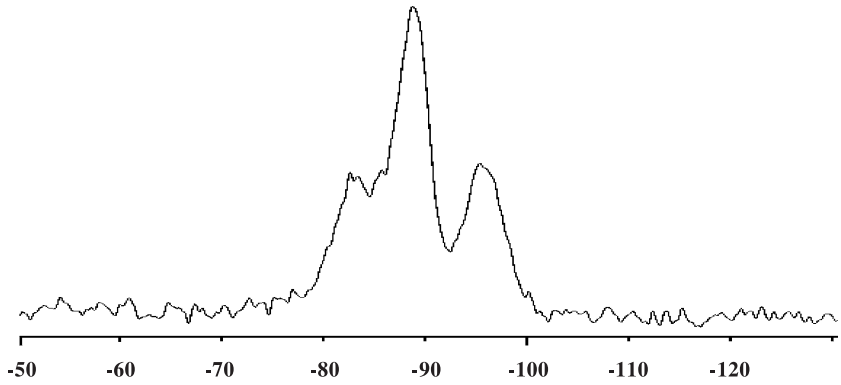

Fig. 7. {^{1}H–^{29}Si} CP-MAS NMR spectrum of M-S-H Gel 2 (Mg/Si = 0.75).

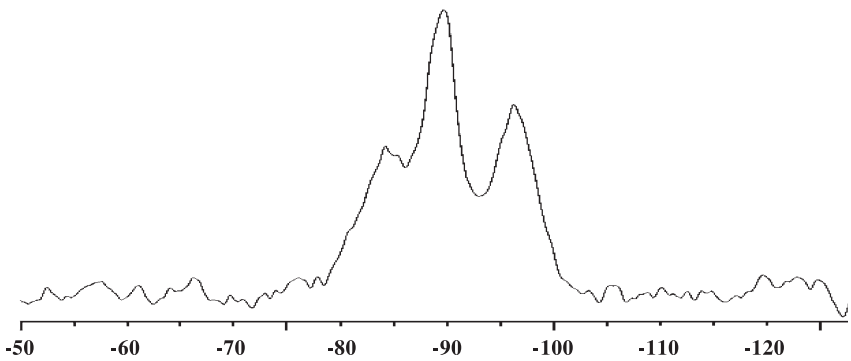

Fig. 8. ^{29}Si MAS NMR spectrum of M-S-H Gel 5 (Mg/Si = 0.96).

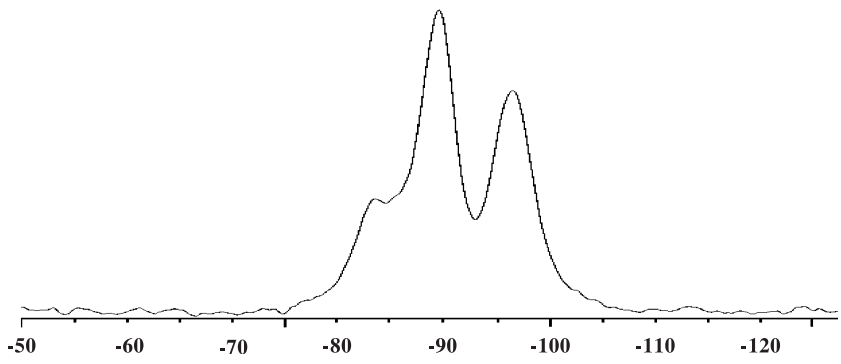

Fig. 9. {^{1}H–^{29}Si} CP-MAS NMR spectrum of M-S-H Gel 5 (Mg/Si = 0.96).

3. Results

3.1. Chemistry and physical structure

Analysis of the supernatant liquids for each synthesis revealed unreacted precursors, resulting in disparate target and analysed solid Mg/Si ratios. Table 1 collates the target Mg/Si ratios of each preparation with the observed values obtained from the solid by EDX. The synthetic gels had mean Mg/Si ratios extending over the range of 0.66–0.96, a considerably narrower range than the target. Fig. 1 displays TEM micrographs of fresh M-S-H Gel 4 which is typical of the state of flocculation of other gels. The micrographs illustrate that M-S-H Gel 4 is composed of agglomerates of particles similar to those known to occur in synthetic C-S-H gel [5].

3.2. XRD characterisation of fresh M-S-H gels cured for 24 h at 20–25 °C

Fig. 2 presents the X-ray diffractogram of two fresh M-S-H gels cured at 20–25 °C; essentially identical patterns were obtained for all gels in both curing conditions and confirm that brucite did not coprecipitate in quantities sufficient to be detected by XRD. In each case, the three major broad peaks evident at 3.6–3.0 Å (25–30°2θ), 2.6–2.3 Å (35–39°2θ) and 1.6–1.5 Å (58–62°2θ) were assigned to M-S-H gel, based on previously reported work [6–9]: values in parentheses are for CuKα radiation. While the 2θ range of the broad peak at 3.6–3.0 Å compares reasonably well with that of amorphous silica, its coprecipitation with M-S-H gels is very unlikely, as will be shown from FT-IR and ^{29}Si NMR evidence presented subsequently as well as chemical analysis of supernatant liquids of silica-rich target compositions (see Table 2) showing that silica not precipitated in M-S-H gel remains in solution.

3.3. FT-IR characterisation of fresh M-S-H gels cured for 24 h at 20–25 °C

Fig. 3 illustrates the FT-IR spectra of fresh M-S-H Gels 1–5 and Table 3 collates the FT-IR spectral data. Data from the FT-IR spectra of all the synthetic M-S-H gels are compared with the spectra of 2:1 M-S-H minerals, sepiolite, $Mg_4[Si_2O_5]_3(OH)_2{\cdot}4H_2O$ and talc, $Mg_3[Si_2O_5]_2(OH)_2$; of the 1:1 M-S-H mineral, serpentine, approximately $Mg_3[Si_2O_5](OH)_4$ and of synthetic M-S-H gels reported by other authors in order to facilitate their characterisation. FT-IR discloses the presence of hydroxyl groups, Mg–OH species, the value of n for Q^n silicon sites and the absence of sorptions attributable to either or both silica gel and brucite. Reported studies [9–14] have shown that the characteristic Mg–OH stretch of phyllosilicates is observed near 3690 cm^{-1}. Each gel exhibits a weak stretch in the reported Mg–OH region but it is important to note the absence of a sharp absorbance near 3720 cm^{-1} attributable to brucite, $Mg(OH)_2$. An additional strong absorption near 3400 cm^{-1} is ascribed to H-bonding and a weak band near 1600 cm^{-1} is ascribed to a hydroxyl stretch. A reported characteristic Si–O vibration (Q^3) for 2:1 phyllosilicate occurs about 1218 cm^{-1} [10] but not all authors agree on this assignment. Nevertheless, very weak absorptions near 1220 cm^{-1} are attributed to Q^3 Si–O vibrations and reflect the poor degree of silica polymerisation in fresh M-S-H gels. The very strong band at 1017 cm^{-1}, with shoulders at approximately 1057 and approximately 904 cm^{-1}, is ascribed to Si–O stretching vibrations at Q^2 sites. A further Si–O stretching at 788 cm^{-1} is due to Q^1 tetrahedra; Si–O–Si bending vibrations account for the absorptions near 690–750 cm^{-1}. Bands near 550 cm^{-1} are assigned to internal deformation of SiO_4 tetrahedra while Mg–O vibrations occur at 472 and 432 cm^{-1} [8,10–14].

3.4. ^{29}Si MAS and {^{1}H–^{29}Si} CP-MAS NMR characterisation of fresh M-S-H gels cured for 24 h at 20–25 °C

Figs. 4–9 illustrate the ^{29}Si MAS and {^{1}H–^{29}Si} CP-MAS spectra for M-S-H Gels 1, 2 and 5 but spectral data for all five fresh gels are given in Table 4: assignment of resonances are made relative to tetramethylsilane (TMS). Broad Q^1 and Q^2 resonances indicate the poorly ordered nature of the gels. Resonances near −100 ppm are assigned

Table 4
Summary of ^{29}Si NMR data of fresh M-S-H Gels 1–5 aged for 24 h at 25 °C

M-S-H gel (Mg/Si)	^{29}Si MAS δ values (ppm)			{^{1}H–^{29}Si} CP-MAS δ values (ppm)		
	Q^1	Q^2	Q^3	Q^1	Q^2	Q^3
1 (0.66)	−84.8 (***p***)	−88.8 (***p***)	−94.8 (***sh***)	−84.0 (***p***)	−88.8 (***p***)	−94.9 (***p***)
			−97.9 (***p***)			−97.9 (***sh***)
2 (0.75)	−83.3 (***p***)	−85.4 (***sh***)	−95.4 (***p***)	−82.7 (***p***)	−85.2 (***sh***)	−95.8 (***p***)
		−89.0 (***p***)	−96.3 (***sh***)		−89.0 (***p***)	−96.7 (***sh***)
3 (0.80)	−84.2 (***p***)	−85.8 (***sh***)	−95.8 (***p***)	−83.6 (***p***)	−85.7 (***sh***)	−95.7 (***p***)
		−89.2 (***p***)	−96.7 (***sh***)		−88.9 (***p***)	−96.8 (***sh***)
			−99.4 (***sh***)			−99.1 (***sh***)
4 (0.90)	−84.0 (***sh***)	−89.1 (***p***)	−96.5 (***p***)	−83.7 (***p***)	−89.6 (***p***)	−96.2 (***p***)
	−85.1 (***p***)			−85.4 (***sh***)		
5 (0.96)	−83.9 (***p***)	−90.0 (***p***)	−96.5 (***p***)	−83.5 (***p***)	−89.8 (***p***)	−96.5 (***p***)
	−85.4 (***p***)			−85.6 (***sh***)		

Key: ***p***—peak; ***sh***—shoulder.

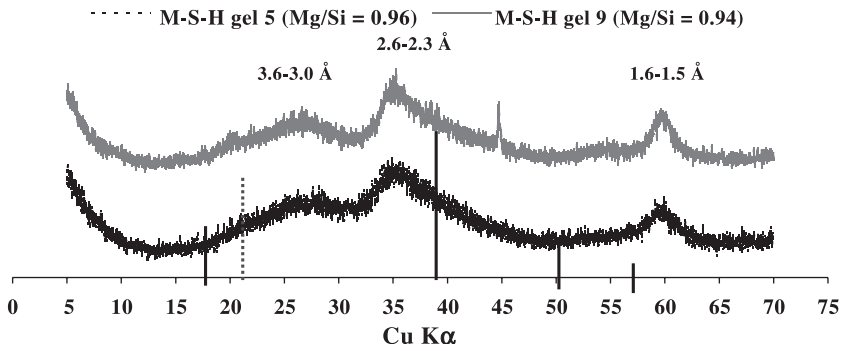

Fig. 10. XRD spectra of M-S-H Gel 5 (fresh) and M-S-H Gel 7 (aged). Black and broken lines denote relative intensities of major reflections for brucite and silica, respectively.

to Q^3 silicon environments. Note that the absence of a Q^4 resonance located near −110 ppm confirms that coprecipitation of silica did not occur.

M-S-H Gel 1 (Mg/Si = 0.66) has a single Q^1 resonance at −84.8 ppm and a Q^2 resonance at −88.8 ppm; a Q^3 resonance is located at −97.9 ppm with a shoulder at −94.8 ppm. Gel 2 (Mg/Si = 0.75) has a Q^1 resonance at −83.3, a Q^2 resonance at −89.0 ppm shouldered by one at $\delta = -85.4$ ppm and two Q^3 resonances at −95.4 ppm (peak) and −96.3 ppm (shoulder) giving M-S-H Gel 2 a total of 5 silicon environments. M-S-H Gels 3–5 have 6, 4 and 4 silicon environments, respectively: their Q^1 and Q^2 δ values compare well to M-S-H Gels 1 and 2 but the chemical shifts of the main Q^3 resonances vary slightly between samples, implying slight structural differences in Q^3 environments; these will be discussed.

3.5. Aged M-S-H gels cured for 6 months at 85 °C

After ageing for 6 months at 85 °C, X-ray powder diffraction studies showed a slight but significant improvement in the degree of crystallinity of each gel in terms of peak half-width, separation and resolution. Fig. 10 displays the XRD spectra isochemical of M-S-H Gels 5 and 9 for comparison. Their appearance suggests the internal structure of the aged gels does not significantly differ from the fresh gels. However, the X-ray powder patterns tend to reflect structural organisation over relatively large distances, 100–1000 Å or more: ^{29}Si NMR and FT-IR, on the other hand, are sensitive to smaller-scale structures and this evidence suggests that significant local structural evolution has occurred. The comparison serves to highlight the limitations of using XRD to characterise materials in which structural changes may be occurring at the nanoscale. Moreover, it is believed that ageing also improves the chemical homogeneity of each composition, as will be shown.

Fig. 11 displays a histogram showing the distribution of Mg/Si ratios in the fresh and aged M-S-H gels determined by EDX. Amongst fresh gels, the data scatter is largest for Gels 1–3: possibly also 5 if the outlier is considered but scatter is generally much reduced when the gels are cured for 6 months. Thus studies with EDX demonstrate improved homogeneity in the M-S-H gels aged at 85 °C for 6 months.

3.6. FT-IR characterisation of aged M-S-H gels cured for 6 months at 85 °C

Fig. 12 illustrates the FT-IR spectra of M-S-H Gels 6–9 and Table 5 collates the FT-IR spectral data. The spectra

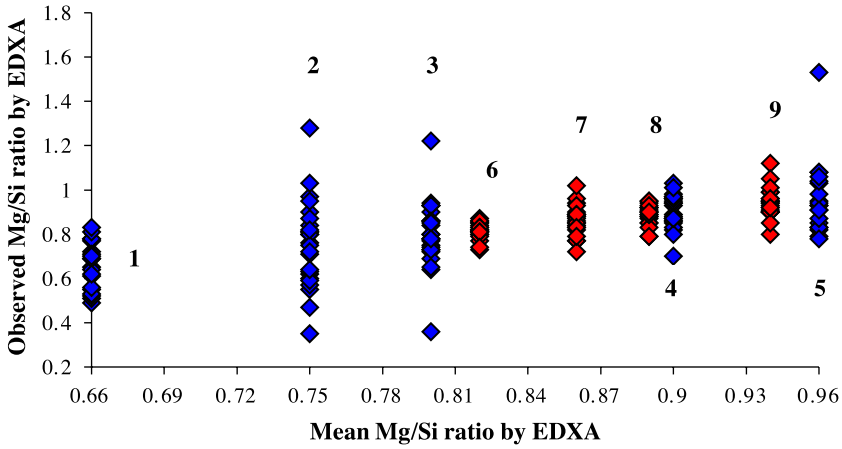

Fig. 11. Histogram of the Mg/Si ratio analysis distribution of fresh M-S-H Gels 1–5 and Aged Gels 6–9. Gels are numbered on chart.

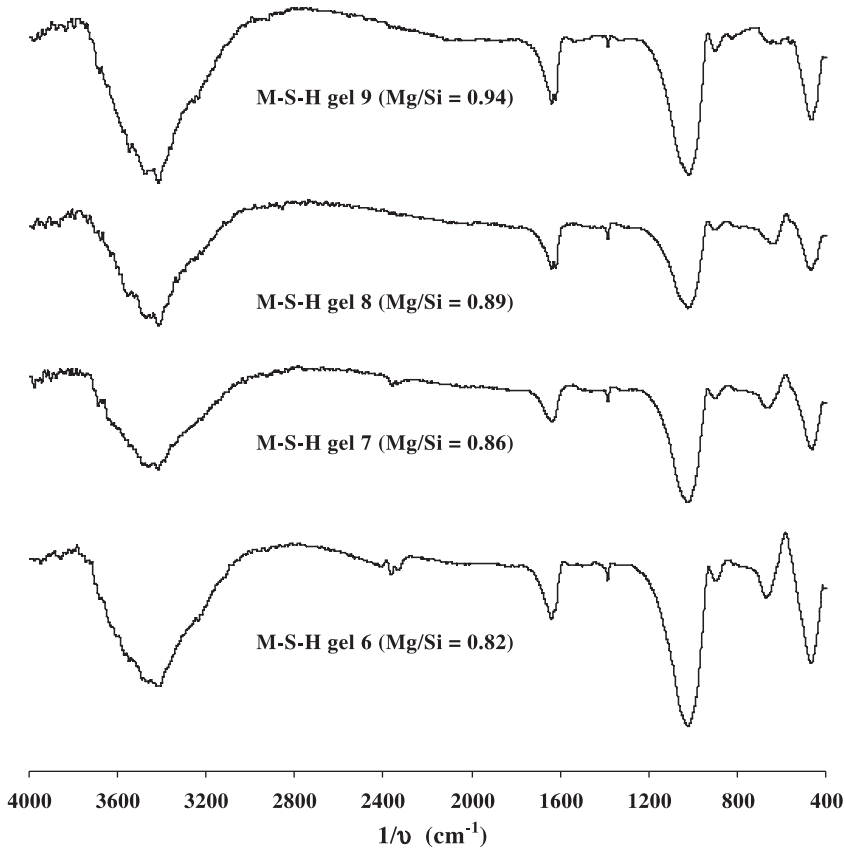

Fig. 12. FT-IR spectra of M-S-H Gels 6–9. Each sample was mixed and pressed with KBr. Absorptions near 2400 cm^{-1} are artefacts due to air contamination.

differ in resolution from those of the equivalent fresh Gels 1–5. In general, the absorption due to Si–O stretching vibrations near 1030 cm^{-1} is sharper, more prominent and development of the hydroxyl band near 1400 cm^{-1} is improved in aged gel relative to the fresh equivalent. Stretching vibrations due to Q^1 environments also occur

Table 5
FT-IR data of aged M-S-H Gels 6–9

M-S-H gel (Mg/Si)	OH vibrations (cm^{-1})	Si–O vibrations (cm^{-1})	Mg–O vibrations (cm^{-1})
6 (0.82)	3414 **s** (H-bonding)	1020 **s** (Q^2 str)	464 **m** (str)
	1638 **m** (OH stretching)	897 **w** (Q^2 bdg)	
	1384 **w** (OH bending)	817 **w** (lattice str)	
		690 **w** (Q^1 str)	
		667 **m** (Q^1 bdg)	
7 (0.86)	3415 **s** (H-bonding)	1021 **s** (Q^2 str)	460 **m** (str)
	1638 **m** (OH stretching)	900 **w** (Q^2 bdg)	
	1384 **w** (OH bending)	815 **w** (lattice str)	
		690 **w** (Q^1 str)	
		667, 654 **m** (Q^1 bdg)[#]	
8 (0.89)	3416 **s** (H-bonding)	1070, 1020 **s** (Q^2 str)	634 **m** (bdg)
	1639, 1619 **m** (OH stretching)	898 **w** (Q^2 bdg)	557 **w** (bdg)
	1384 **w** (OH bending)	815 **w** (lattice str)	465 **m** (str)
		790 **w** (Q^1 bdg)	
		687 **w** (Q^1 str)	
		665**m** (Q^1 bdg)	
9 (0.94)	3837 **m** (H-bonding)	1050, 1017 **s** (Q^2 str)	560 **w** (bdg)
	3679 **m** (OH stretching)	900 **w** (Q^2 bdg)	462 **m** (str)
	3649, 3415 **s** (H-bonding)	823 **w** (lattice str)	
	1638, 1620 **m** (OH stretching)	690 **w** (Q^1 str)	
	1384 **w** (OH bending)	649, 617 **w** (Q^1 bdg)[#]	

Key: **s**—strong; **m**—medium; **w**—weak; str—stretching vibration; bdg—bending vibration.
[#] Doublet.

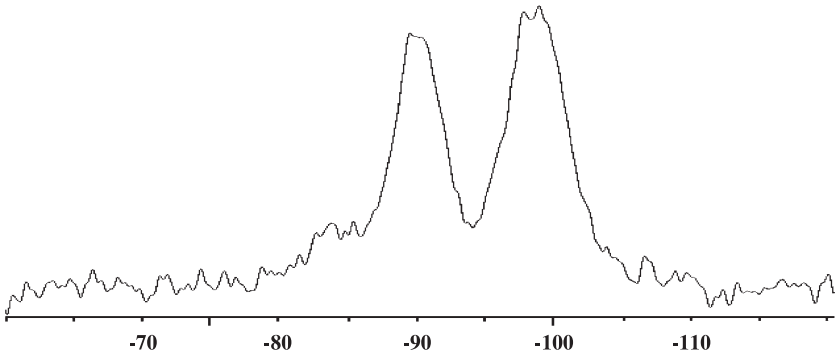

Fig. 13. ^{29}Si MAS NMR spectrum of M-S-H Gel 6 (Mg/Si = 0.82).

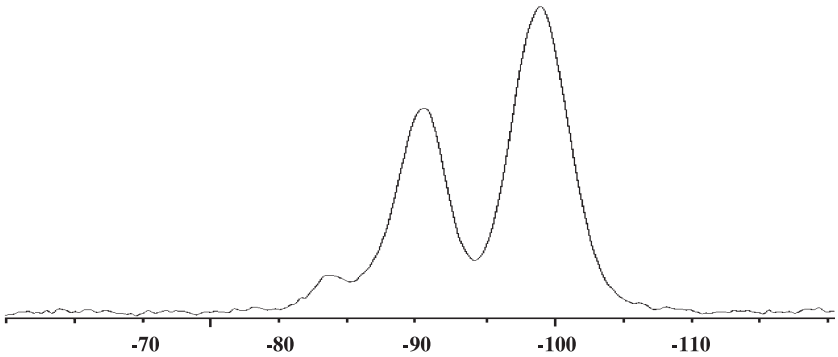

Fig. 14. {^{1}H–^{29}Si} CP-MAS NMR spectrum of M-S-H Gel 6 (Mg/Si = 0.82).

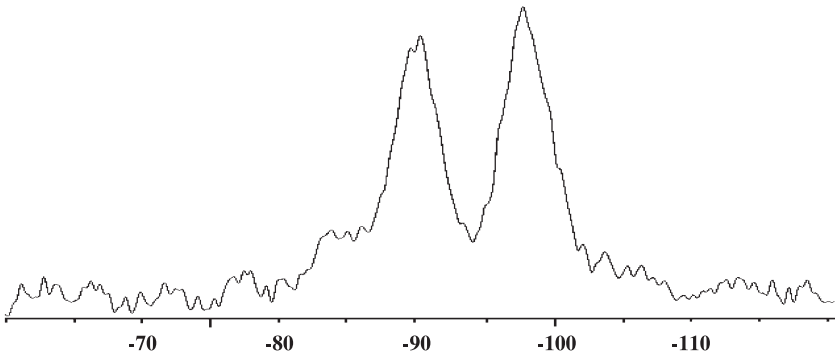

Fig. 15. ^{29}Si MAS NMR spectrum of M-S-H Gel 8 (Mg/Si = 0.89).

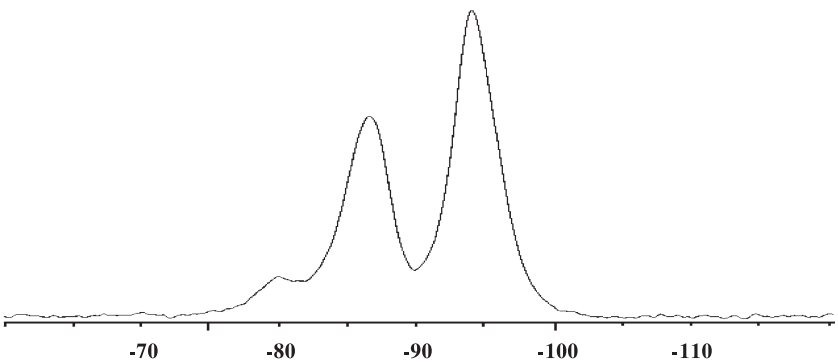

Fig. 16. {^{1}H–^{29}Si} CP-MAS NMR spectrum of M-S-H Gel 8 (Mg/Si = 0.89).

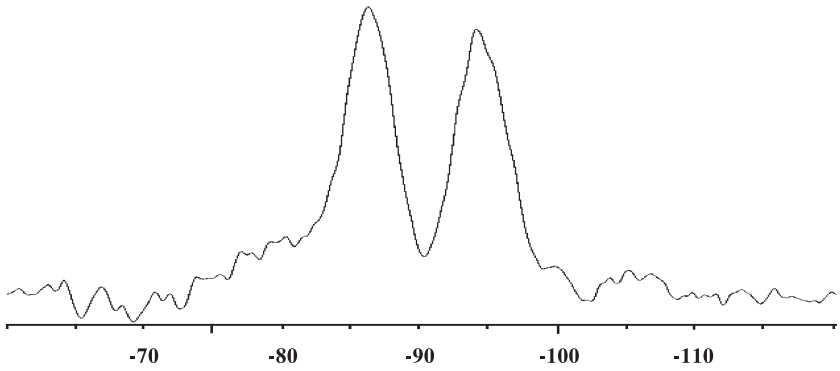

Fig. 17. ^{29}Si MAS NMR spectrum of M-S-H Gel 9 (Mg/Si = 0.94).

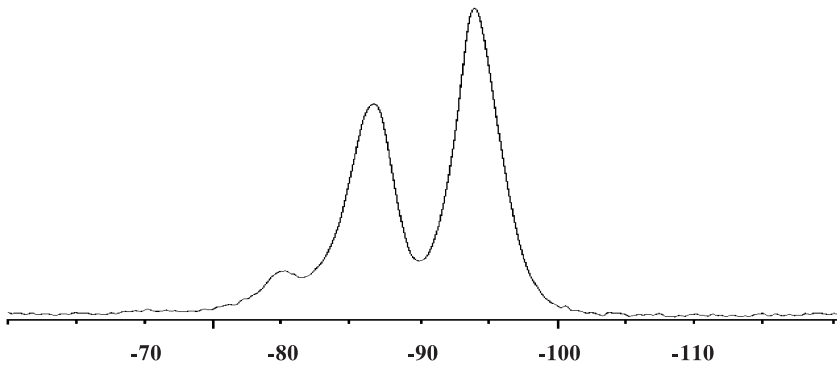

Fig. 18. {^{1}H–^{29}Si} CP-MAS NMR spectrum of M-S-H Gel 9 (Mg/Si = 0.94).

near 800 cm^{-1}. However, unlike M-S-H Gels 1–5, Si–O stretching vibration bands near 1200 cm^{-1}, indicating the presence of Q^3 silicon sites, were not observed despite ^{29}Si NMR evidence of the existence of Q^3. According to some authors, FT-IR spectra of M-S-H minerals show little absorption in this region [12,15]. Therefore, the absence of absorptions at approximately 1200 cm^{-1}, which might have been expected to give some indication about the improved structural characteristics of M-S-H Gels 6–9, is probably inconclusive. M-S-H Gels 6 and 7 exhibit very similar FT-IR patterns. However M-S-H Gel 7 displays another feature: typical trioctahedral Si–OH deformation doublet bands are present at 667 and 654 cm^{-1}. These are not present in Gel 6, perhaps due to overlap with other features, but are present in the spectra of M-S-H Gels 7 and 9. FT-IR (and ^{29}Si NMR, presented subsequently) data also confirm that the local ordering has been improved by ageing for approximately 6 months at 85 °C.

3.7. ^{29}Si MAS and {^{1}H–^{29}Si} CP-MAS NMR characterisation of M-S-H gels cured for 6 months at 85 °C

The ^{29}Si NMR spectra for M-S-H Gels 6, 8 and 9 are displayed in Figs. 13–18. Using identical NMR parameters as for the fresh gels, each MAS spectrum still has a large signal/noise ratio but the peak definition is improved compared with M-S-H Gels 3–5: Table 6 collates the corresponding MAS and CP-MAS data.

The substantial and significant reduction in intensity of the Q^1 resonances in aged gels compared with those of the corresponding fresh gels illustrates the ageing process much better than either XRD or FT-IR: nearly all the unpolymer-

Table 6
Summary of ^{29}Si NMR data for M-S-H Gels 6, 8 and 9

M-S-H gel (Mg/Si)	^{29}Si MAS δ values (ppm)			{^{1}H–^{29}Si} CP-MAS δ values (ppm)		
	Q^1	Q^2	Q^3	Q^1	Q^2	Q^3
6 (0.82)	−84.0 (***p***)	−89.3 (***p***)	−98.8 (***p***)	−84.1 (***p***)	−90.9 (***p***)	−98.7 (***p***)
8 (0.89)	−83.1 (***sh***)	−89.6 (***sh***)	−97.7 (***p***)	−80.1 (***p***)	−86.9 (***p***)	−94.3 (***p***)
	−84.0 (***p***)	−90.6 (***p***)				
9 (0.94)	−80.3 (***p***)	−86.4 (***p***)	−94.6 (***p***)	−80.3 (***p***)	−86.9 (***p***)	−94.0 (***p***)

Key: ***p***—peak; ***sh***—shoulder.

ised species combine in the course of ageing to produce polymerised Q^2 and Q^3 species. The relative proportions of Q^3/Q^2 also increase, indicating enhancement in the number of Q^3 silicon sites and progressive structural polymerisation. Gel 6 has a peak at −89.3 ppm which is tentatively attributed to Q^2. However, this signal is very close to the Q^3 chemical shift range and it may be a Q^3 resonance shifted upfield due to structural distortion. Gel 6 has different Q^1, Q^2 and Q^3 chemical shifts relative to Gels 8 and 9, suggesting that is has a unique internal structure. Gel 8 has a Q^2 peak at −90.6 ppm with a shoulder at −89.6 ppm, as well as two Q^1 resonances, suggesting it has the poorest homogeneity. In the CP-MAS spectrum of Gel 8, the chemical shifts of the Q^2 and Q^3 peak resonances are different compared to the corresponding features in the MAS spectrum. The differences imply that the protons are close to Q^2 and Q^3 silicon sites. Alternatively, the large Q^1 peak might be overlapped by other Q^1 resonances. Gel 9 has a single Q^2 shift at −86.4 ppm, suggesting improved homogeneity compared to Gels 6 and 8. Visually, the Q^2/Q^3 ratio for Gel 9 is larger than in Gels 6 and 8, implying that the structure of Gel 9 has developed the least in the course of ageing.

Despite having narrow Mg/Si ratios, gels within one series, fresh or aged, exhibit Q^3 peaks with different chemical shifts implying composition-dependent structural characteristics. The differences are in general greater for aged gels despite their smaller composition range.

4. Discussion

Considerable divergence of views exists in the literature concerning the mineralogical role of Mg in cements, introduced both from cement clinker or in supplementary cementing materials, e.g., slag, or as Mg introduced from the service environment. The situation concerning which Mg phase or phases develop is relatively simple. In the first case, of Mg in cement materials, Mg is relatively insoluble in C-S-H phases and must, therefore, form an independent phase or phases containing essential magnesium. On the other hand, none of the potential candidate magnesium-containing phases include significant calcium. The chemical and mineralogical nature of the magnesium phase or phases is a function of silica and alumina activities: at low activities of both silica and alumina, brucite, $Mg(OH)_2$, is the favoured product. However, blended cements with silica fume, fly ash or slag are characterised by higher silica and/or alumina activities than Portland cement, favouring mixtures of brucite with M-A-H and/or M-S-H phases: brucite may be totally reacted. In external Mg attack, brucite typically appears in the altered surface layers on concrete undergoing external sulfate attack because the attacking solutions tend to have high ratios of $[MgO]/[Al_2O_3 + SiO_2]$. As alumina and silica activities increase, as occurs at depth within unaltered or slightly altered cement and blended cements, hydrotalcite and M-S-H gel appear, often together with brucite. The relative amounts of phases depend in part on the amounts of silica and alumina available for reaction, so the appearance of M-A-H and M-S-H phases is enhanced by the presence of slag, fly ash, metakaolin, etc. which contribute one or more essential components of M-A-H and M-S-H phases. While the hydrotalcite-like M-A-H phase is comparatively well characterised, less attention has been devoted to the M-S-H phase, its composition, structure and the impacts of time and temperature on its constitution. To aid our discussion, Fig. 19 illustrates the two windows of study of M-S-H gel formation reported in this paper: one, a short cure at 20–25 °C, and the other, a long cure at 85 °C. It is not certain if changes in the state of M-S-H gels between the two datasets are due to time, temperature or both. Clearly, this will have to be addressed in future studies. However, presently available data are sufficient to characterise the M-S-H phase.

M-S-H gels were precipitated to give a range of target Mg/Si ratios from 0.5 to 1.5 to probe the limits of single product M-S-H gel formation. Ratios either matching or close to known M-S-H minerals: sepiolite, $Mg_4[Si_2O_5]_3(OH)_2{\cdot}4H_2O$ (Mg/Si = 0.67); talc, $Mg_3[Si_2O_5]_2(OH)_2$ (Mg/Si = 0.75) and serpentine, $Mg_3[Si_2O_5](OH)_4$ (Mg/Si = 1.0) were included deliberately to serve as benchmarks during the characterisation stage. However, M-S-H products with low target Mg/Si ratios (Mg/Si = 0.5, 0.6 and 0.75), precipitated with higher than expected ratios while the Mg/Si ratios of the remaining syntheses were lower than the target ratios. Thus, the actual compositions of the gels ranged rather narrowly, between Mg/Si = 0.66 and 0.96 (see Table 1). These synthesis limits may not represent the maximum possible extent of M-S-H gel formation but it appears probable that, relative to C-S-H gels, M-S-H gels do not extend to Mg/Si ratios exceeding 1.0. Although it is believed that the fresh gels are notably inhomogeneous, as will be discussed, we tentatively conclude that M-S-H gels outwith this narrow band of compositions, Mg/Si 0.66 to 1.0 approximately, are not persistent.

XRD confirmed that the precipitates were gel-like by the definition given earlier; that is, an apparently single phase of

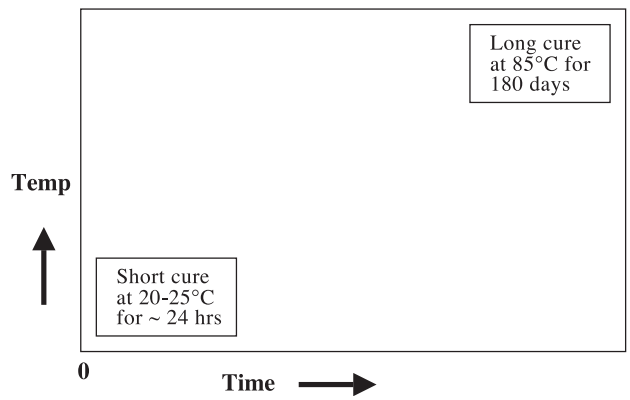

Fig. 19. Two "windows" of study: one at short cure and one at long cure.

low crystallinity was obtained, structurally intermediate between a true gel and a crystalline phase. FT-IR showed that the gels had a low degree of polymerisation but contained more or less all the generic stretches associated with M-S-H compounds.

The nature of the quasi-crystalline component of gels is composition dependent. From all the evidence, the crystalline component of M-S-H Gel 1 has a sepiolite-like character. We note that the Mg/Si ratio of Gel 1, by EDX, is 0.66—within limits of experimental error—identical to that of sepiolite (0.67). In support of this, an FT-IR absorption band near 1600 cm^{-1}, assigned by Singer et al. [10] to channel water co-ordinated to the Mg^{2+} ions at the edges of the 2:1 layers of sepiolite, is also present in gel spectra. Additional absorption bands characteristic of 2:1 phyllosilicates occur near 1220 cm^{-1}, albeit very weak. Further supportive evidence for some sepiolite-like character lies with the ^{29}Si NMR spectrum: diagnostic Q^3 resonances for sepiolite are located at −92.0, −95.0 and −98.5 ppm and these compare with resonances actually found at −94.9 and −97.9 ppm. The differences in shift are ascribed to the low polymerisation state of the gel, given the absence of other cationic substitutions which might influence the NMR.

M-S-H Gel 2 has a Mg/Si ratio of 0.75—identical to that of talc, $Mg_3[Si_2O_5]_2(OH)_2$—and on that account might be supposed to have some talc-like character. The major Si–O vibrations of natural talc absorb at 1045, 1018 and 670 cm^{-1} and these compare reasonably well with those observed for Gel 2, having absorptions at 1033, 1014 and 670 cm^{-1}. Note that talc has no interlayer water; thus, the intensity of its hydrogen bond vibrations is ideally absent but is in practise weak. Indeed, the main OH vibration of Gel 2, at 3414 cm^{-1}, shows reduced intensity: the assignment is as would be expected of a talc-like structure relative to sepiolite. Gel 2 also exhibits Mg–O stretching absorptions at 551, 472 and 417 cm^{-1} of medium intensity; the assignment is based on the work reported by Weiss et al. [16]. These are unique to talc. The diagnostic Q^3 resonance of talc is located at −97.0 ppm compared to a peak at −95.8 ppm and shoulder at −96.7 ppm for M-S-H Gel 2 as reported in this paper: NMR thus agrees with the evidence obtained from FT-IR in support of a talc-like nanostructure.

The spectra of M-S-H Gels 3 and 4 have two Si–O vibrations near 1030 cm^{-1} with a shoulder at about 1080 cm^{-1}. The shape of this band is different to the corresponding band of Gels 1 and 2 and is more indicative of a 1:1 layer phyllosilicate-like structure, such as serpentine. However, the ^{29}Si NMR resonances do not compare well with those of serpentine because Gel 3 gives rise to three signals, all considerably further upfield than the diagnostic single serpentine Q^3 shift at −92 ppm. FT-IR data for well-crystallised serpentine were reported by Caillerie et al. [15]; its principal absorption occurred at 1045, 1015, 962 and 615 cm^{-1}, and these do relate reasonably well to those of Gel 5. The FT-IR spectra of M-S-H gels prepared by Caillerie et al. [8] and Temuujin et al. [6,7], made using a similar preparative method to that of the title paper, show absorptions near 1030, 900, 800, 657 and 470 cm^{-1} and these correlate well with those observed in the title study. Both authors assign the FT-IR bands at 910 and 630 cm^{-1} to the Mg–OH bending vibrations in a magnesium silicate layer structure. Poorly crystalline trioctahedral M-S-H gels were prepared hydrothermally by Speakman and Majumdar [15] in a pioneering FT-IR study: the gels exhibited absorption bands near 880 cm^{-1} which correspond to the absorption found generally in Gels 1–9. It is concluded that Gels 3 and 4 display characteristics of both 2:1 and 1:1 phyllosilicates: that is, they are mixtures of two crystalline nanoscale phases embedded in a relatively amorphous matrix.

A long cure, 6 months at 85 °C, brings several changes compared to the short cure, approximately 25 °C. For example, the FT-IR data are sharper and more detailed as a result of improved structural development. Fig. 11 shows how the range of Mg/Si ratios narrows as the curing time and temperature are increased. XRD shows that Gels 6–9 are still poorly ordered and crystals large enough to be detected by conventional XRD have not formed, although their FT-IR spectra resemble that of poorly crystalline talc prepared by other authors [8,17]. This poorly crystalline talc gives rise to characteristic strong absorption bands at 1018, 670 (Q^3 Si–O vibrations), 467 and 452 cm^{-1} (both Mg–O vibrations), all of which are enhanced by the longer cure duration. According to Farmer [13], Si–O vibrations occurring near 1000, 790 and 660 cm^{-1} are characteristic of 2:1 type phyllosilicates. The FT-IR vibrations of a 2:1 phyllosilicate compare reasonably well the with the ^{29}Si NMR data for Gel 6: the spectrum shows a single resonance at −98.7 ppm compared with that of crystalline talc, at −97 ppm. Note that M-S-H Gel 7 displays a doublet at 600–700 cm^{-1} characteristic of a 2:1 trioctahedral phase, corroborating the supposition that ageing improves the local structural order, the nature of which is also sensitive to Mg/Si ratio.

While M-S-H Gels 8 and 9 exhibit many of the bands observed for M-S-H Gels 6 and 7, they also exhibit different features: only one part of the characteristic 2:1 trioctahedral doublet is present in their FT-IR spectrum. There are some bands attributable to 2:1 phyllosilicates (3632, 3557 and 1619 cm^{-1}), but bands associated with semicrystalline serpentine also occur: for example, an absorption band of medium intensity at 630–580 cm^{-1}. Gels partaking of structural features typical of both 2:1 and 1:1 phyllosilicate character have been termed *deweylite* by Speakman et al. [15], who defined deweylite as a poorly crystalline magnesium silicate hydrate with a variable composition whose Mg/Si ratio lies between those of talc (Mg/Si = 0.75) and serpentine (Mg/Si = 1.5). Such mixtures are said to form naturally in hydrating Portland cements high in MgO [15]. While the term deweylite has been discredited as a proper mineral name, it still usefully describes the structural state of gels in the appropriate range of compositions.

Note that M-S-H Gel 9 shows absorption bands that are typical of serpentine minerals, i.e., 1:1 trioctahedral phyllosilicates. The vibrations of chrysotile absorb near 3640, 3390 (OH bending vibrations), 1613 cm^{-1} (OH stretching vibration), 1081, 1015 and 620 cm^{-1} (Si–O stretching vibrations) [11,12]. These compare reasonably well with the FT-IR data of Gel 9, as collated in Table 5. The ^{29}Si NMR data show single resonances near −94 ppm which more resemble 1:1 phyllosilicates, such as chrysotile (−92 ppm), than 2:1 phyllosilicates, such as talc (−97 ppm).

In summary, two windows of study of M-S-H gel formation and corresponding structural states are reported in this paper: one resulting from a short cure at 20–25 °C, the other from a long cure at 85 °C. XRD and ^{29}Si NMR disclosed that the freshly precipitated gels were poorly crystalline. The differences in relative intensities of the Q^1, Q^2 and Q^3 resonances indicated the gels had individual, composition-dependent polymerisation and structural characteristics. M-S-H Gel 1 (Mg/Si = 0.66) and Gel 2 (Mg/Si = 0.75) show strong similarities to sepiolite (Mg/Si = 0.67) and talc (Mg/Si = 0.75), respectively, by EDX, FT-IR and ^{29}Si NMR. The character of Gels 3–5 appeared to be intermediate to those of 2:1 and 1:1 phyllosilicates and may, therefore, consist of phase mixtures. It is envisaged that nanoscale "islands" of more crystalline matter are embedded in an amorphous, or nearly so, matrix.

The ageing of gels for 6 months at 85 °C resulted in increased polymerisation and enhanced structural development of the crystalline at the expense of gel: in particular, Q^1 sites appeared to polymerise to Q^2 and Q^3 sites, as demonstrated by larger Q^3 intensities relative to Q^1 and Q^2 intensities, and the resolution of FT-IR peaks was sharper. However, the aged products remained poorly ordered by XRD; hence, crystallinity fails to develop beyond the nanoscale range. The range of Mg/Si ratios narrowed compared with M-S-H Gels 1–5. The analytical data showed both 2:1 and 1:1 phyllosilicate character which is ascribed to a mixed layer deweylite-like structure, i.e., originating from a poorly crystalline magnesium silicate hydrate with a variable composition whose Mg/Si ratio lies between those of talc (Mg/Si = 0.75) and serpentine (Mg/Si = 1.5).

Finally, it is appropriate to comment on two other aspects of gel structure: the state of crystalline regions and the relation between M-S-H and C-S-H gels. Although structural units have been suggested to exist in M-S-H gels, and the nature of such units to depend on Mg/Si ratio, it is apparent from the low Q^n numbers found by ^{29}Si NMR that much amorphous material is retained in fresh and annealed preparations. It is further suggested that the overall structure appears to vary continuously with composition but that the volume fraction of the different types of structured regions is sensitive to composition as well as to ageing time and temperature. High-resolution electron microscopy with diffraction is likely to yield direct information on the structural state of these gels and it is suggested that future studies should embrace this aspect. In comparison with C-S-H gels, very similar phenomena occur, although the local crystallochemical structures of C-S-H more closely resemble the layer structures of C-S-H minerals: gyrolite, tobermorite and jennite, or mixtures thereof. On account of the basic structural differences between the nature of ordered regions, the two gel types, M-S-H and C-S-H, are essentially immiscible. This conclusion is supported by several decades of transmission electron microscopy, with analysis and electron diffraction, of matrices, such as slag cement blends. Many analyses in the literature reporting Ca in M-S-H gels and of Mg in C-S-H gels probably result from inability physically to resolve intimate fine-grained mixtures of two gels. Studies of 'structure' within gels and the elucidation of the nature of structural units has been much advanced by application of NMR and its linking to complimentary FT-IR and diffraction studies.

Acknowledgements

The financial support of Nuclear Electric is acknowledged. The opinions expressed here are those of the authors and do not necessarily reflect those of Nuclear Electric. The authors would like to thank Dr. Sandy Chudek, University of Dundee for assistance with NMR and Dr. Eric Lachowski for assistance with electron microscopy and diffraction.

References

[1] D. Bonen, M.D. Cohen, Magnesium sulfate attack on Portland cement paste: I. Microstructural analysis, Cem. Concr. Res. 22 (1992) 169–180.
[2] D. Bonen, M.D. Cohen, Magnesium sulfate attack on Portland cement paste: II. Chemical and mineralogical analyses, Cem. Concr. Res. 22 (1992) 707–718.
[3] W.F. Cole, A crystalline hydrated magnesium silicate formed in the breakdown of a concrete sea-wall, Nature 171 (1953) 354–355.
[4] R.S. Gollop, H.F.W. Taylor, Microstructural and microanalytical studies of sulfate attack: I. Ordinary Portland cement paste, Cem. Concr. Res. 22 (1992) 1027–1038.
[5] S.-Y. Hong, Calcium silicate hydrate: Crystallisation and alkali sorption, PhD Thesis, University of Aberdeen, UK (2000).
[6] J. Temuujin, K. Okada, K.J.D. MacKenzie, Formation of layered magnesium silicate during the aging of magnesium hydroxide–silica mixtures, J. Am. Ceram. Soc. 81 (3) (1998) 754–756.
[7] J. Temuujin, K. Okada, K.J.D. MacKenzie, Role of water in the mechanochemical reactions of $MgO–SiO_2$ systems, J. Solid State Chem. 138 (1998) 169–177.
[8] J.-B. d'E Caillerie, M. de la Kermarec, O. Clause, ^{29}Si NMR observations of an amorphous magnesium silicate formed during impregnation of silica with Mg(II) in aqueous solution, J. Phys. Chem. 99 (1995) 17273–17281.
[9] N. Takahashi, M. Tanaka, M.T. Satoh, T. Endo, Study of synthetic clay minerals: III. Synthesis and characterization of two dimensional talc, Bull. Chem. Soc. Jpn. 67 (1994) 2463–2467.
[10] A. Singer, K. Stahr, M. Zarei, Characteristics origin of sepiolite (Meerschaum) from Central Somalia, Clay Miner. 33 (1998) 349–362.
[11] G.W. Brindley, J. Zussman, Infra-red absorption data for serpentine minerals, Am. Mineral. 44 (1959 Jan.–Feb.) 185–188.
[12] V.C. Farmer (ed.), The Infrared Spectra of Minerals, Mineralogical Society, Adlard & Son, Surrey, UK (1974).

[13] H.W. van der Marel, H. Beutelspacher, Atlas of Infrared Spectroscopy of Clay Mineral and their Admixtures, Elsevier, Amsterdam, 1976, p. 66.
[14] P. Yu, R.J. Kirkpatrick, B. Poe, P.F McMillan, X. Cong, Structure of calcium silicate hydrate (C-S-H): Near-, mid-, and far-infrared spectroscopy, J. Am. Ceram. Soc. 82 (3) (1999) 742–782.
[15] K. Speakman, A.J. Majumdar, Synthetic deweylite, Mineral. Mag. 38 (1971 June) 225–234.
[16] C.A. Weiss Jr., S.P. Altaner, R.J. Kirkpatrick, High-resolution ^{29}Si NMR spectroscopy of 2:1 layer silicates: Correlations among chemical shift, structural distortions and chemical variations, Am. Mineral. 72 (1987) 935–942.
[17] N. Takahashi, M. Tanaka, T. Satoh, T. Endo, Study of synthetic clay minerals: III. Synthesis and characterization of two dimensional talc, Bull. Chem. Soc. Jpn. 67 (1994) 2463–2467.